Chapter V (A)

Assessment of seaweed bioadsorbent (*Fucus vesiculosus*) for removal of methylene blue and rhodamine B dyes

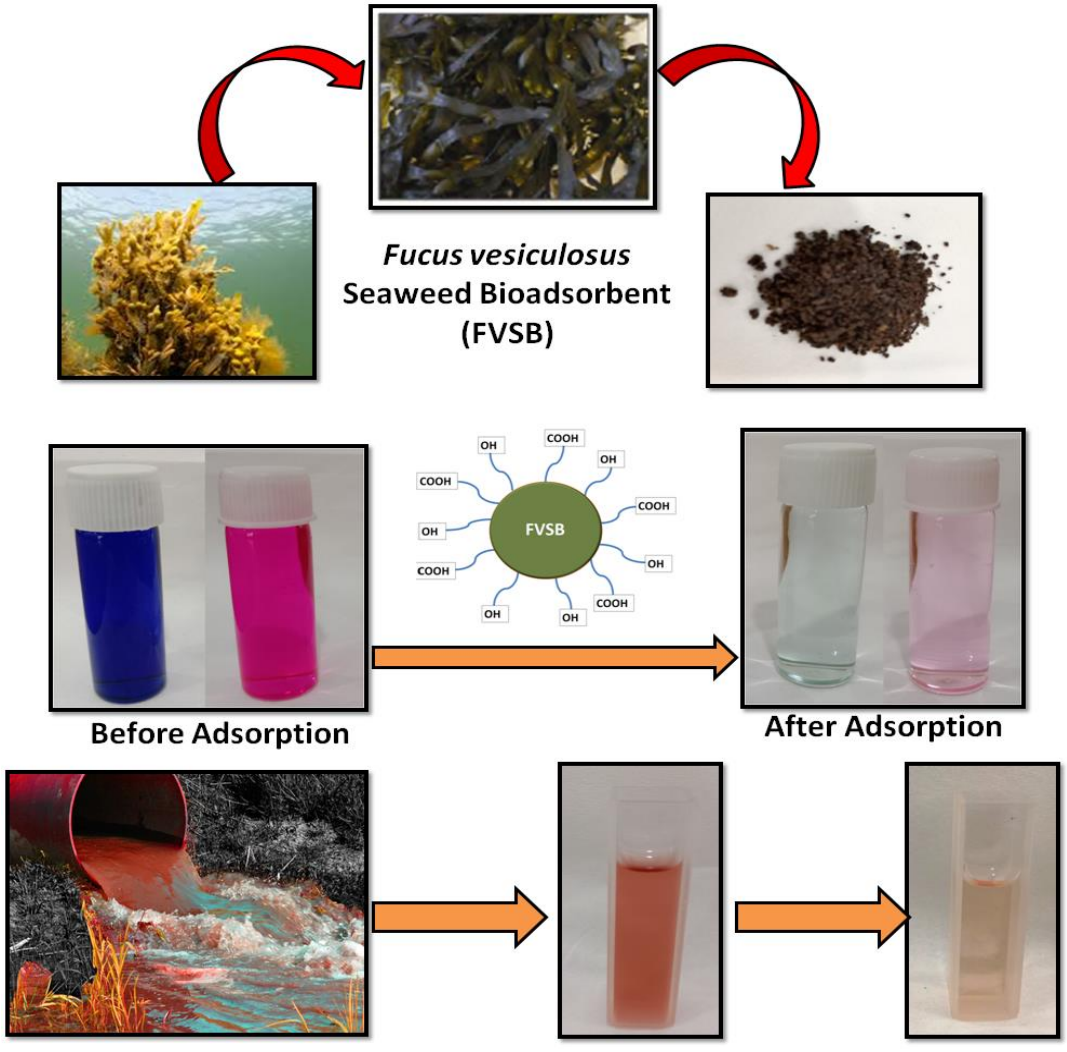

5.1.1. Introduction

Wastewater effluents discharged from various sectors such as agriculture, households and industry contain a variety of organic and inorganic contaminants such as cyanides, heavy metals, phenols, pesticides, and dyes [1,2]. Direct release of these effluents into the natural system without prior treatment degrades the environment that affects flora and fauna as well as humans in the long term[3]. Dyes represent a significant group of organic pollutants present in industrial effluents, as they are used in many areas such as textiles, rubber, pharmacy, food, paper, leather and cosmetics[4]. In addition to the annoying aesthetic nature, the presence of dyes pollutes both surface and groundwater because of their indestructible nature and toxicity. The dyes impart several adverse effects on the environment such as enhancement of chemical oxygen demand of water body, obstruction to the usual photosynthetic activity of aquatic flora and irregular aquatic organism metabolism[5]. Other than imparting colors, dyes could cause severe teratogenic carcinogenic and mutagenic effect[6].

Cationic dye Methylene blue (MB) is broadly utilized in the dyeing of wood, cotton, silk and so on. Various adverse effects such as nausea, burning sensation, skin irritation, vomiting, diarrhoea, eye injury and breathing issues are caused by direct ingestion of MB[7]. Rhodamine B (RB) is an amphoteric dye used as the tracer for determining water flow. Carry out the role of histological dyes, from flurochrome to fluoroprobes, commonly utilized with the fluorometer and application of biotechnology. Ingestion of RB causes gastrointestinal problems, reproductive damage, nose irritation, tongue and skin[8]. Consequently, wastewater treatment before disposal in the natural environment is necessary. There are several reported biological, chemical and physical methods for the elimination of dyes from wastewater such as flocculation and coagulation, adsorption, oxidation process, membrane filtration, nanotechnology, ozonation and ion exchange[9–11]. Adsorption is regarded as the most practical, economical and easy-to-use method of removing dyes from the aqueous solution. In order to eliminate pollutants from wastewater various adsorbents have been reported till date such as hydrogels[12,13], seaweeds[14], polymer-clay[15], agricultural wastes[16], alumina[17], activated graphene oxide[18], bioadsorbents [11,19,20], carbon[21], mesoporous SiO_2[22], aerogels[23,24], MCM-41 and MCA[25] and nanoadsorbent[26].

The bioadsorbents exhibit the advantages of high sorption capacity, ease of availability, regeneration, less financial input, less sludge generation, ecofriendly and harmless nature due to which it gathers the attention of researchers now-a-days for elimination of contaminants from

polluted water [27]. The bioadsorbent has several active functional groups such as carboxyl, hydroxyl and amine groups on its surface, which contributes to a high adsorption capacity[28]. Materials from biological sources and their derivatives could be used to remove pollutants. Recently, marine algae have attracted special attention as bioadsorbent as they have various advantages over other adsorbent system. Depending on the climatic conditions, seaweeds, a form of renewable resource grows easily in fresh and salt water system [29]. Dried seaweed could be stored longer without losing its properties[30]. *Fucus vesiculosus*, a brown macroalgae, is abundant in coastal areas with significant polysaccharides proportion. They are primarily used in foodstuffs, nutritional supplements and cosmetics [31]. Some of the reported environmental remediation studies utilizing seaweeds have been discussed such as single and binary adsorption of reactive blue 4 and reactive orange 16 dyes studied by Thivya et al, utilized *Kappaphycus alvarezii* derived biochar[32]. The report of Laabd et al., represents elimination of crystal violet and congo red dye using green seaweed *Codium decorticatum* alga (CDA) with higher removal efficiency of 96.9% and 89.8%, respectively [33]. Successful removal of methylene blue dye was observed with adsorption capacity of 191.38 mg/g utilizing *Sargassum muticum* seaweed has been reported[34]. Since the simultaneous adsorption of pollutants is important as far as practical applicability is concerned, this study therefore, represents the mono component and the simultaneous adsorption of the dyes in mixture.

In this study, *Fucus vesiculosus*, a brown seaweed has been used as bioadsorbent for elimination of cationic dyes like Methylene Blue and Rhodamine B from their aqueous solution. The presence of various functional groups on *Fucus vesiculosus* seaweed bioadsorbent (FVSB) surface helps in elimination of dyes from single and binary system with high removal efficiency and adsorption capacity. Several techniques such as Thermogravimetric Analysis (TGA), Fourier Transform Infrared Spectroscopy (FTIR), Scanning Electron Microscope (SEM) and Energy dispersive X-ray (EDX) has been utilized for characterization of FVSB. Adsorption parameters such as dosage, pH, concentration and temperature variation have been explored. The experimental data were fitted into adsorption isotherm, kinetics and thermodynamic models. FVSB, successfully remove dyes from their aqueous solution and environmental sample with high removal efficiency and could be used as promising approach for environmental remediation.

5.1.2. Materials and Methods

5.1.2.1.Materials

The seaweed sample of *Fucus vesiculosus* was collected from nearby areas of Amlwch port during the low water tide[35]. Methylene Blue and Rhodamine B were purchased from Fisher Scientific, Navi Mumbai, India. De-ionized water was used for preparation of dye solutions. Analytical grade reagents were used as received.

5.1.2.2. Preparation of *Fucus vesiculosus* Seaweed Bioadsorbent (FVSB)

The collected sample of seaweed was washed thoroughly using distilled water for 3-4 times and sun dried. The dried samples were kept in the oven at 60°C till constant weight was procured. The samples were ground, converted into uniform size and stored for further utilization. Before adsorption study, the seaweed was kept in water to remove color. After decolorization the seaweed sample was dried again till constant weight and used for adsorption study as shown in **Figure 5.1.1**.

Figure 5.1.1: Preparation of bioadsorbent FVSB

5.1.2.3.Characterization of FVSB

FTIR spectra of FVSB as KBr disc was done with PerkinElmer IR spectrophotometer at room temperature. JSM-5000 LV was utilized for the analysis of Scanning Electron Microscopy (SEM) and Energy Dispersive Spectrometer (EDS) of vacuum dried FVSB before and after adsorption. TG–DTA 6300 INCARP EXSTAR 6000 was used for Thermo gravimetric analysis (TGA) of FVSB in the range of 30–500°C and 10°C/min heating rate with nitrogen atmosphere maintained throughout the process. Agilent Technologies Cary 60 UV-vis spectrophotometer was used for UV-vis spectrophotometric measurements.

5.1.2.4. Adsorption of Organic Dyes

The adsorption capacity of FVSB was investigated using two cationic organic dyes i.e. Methylene Blue (MB) and Rhodamine B (RB). 50 mL dye solution was kept in 150 mL conical flask for adsorption process. The optimum concentration of MB and RB dye was determined using the range of 50-250 mg/L with a fixed amount of bioadsorbent. The mixture was kept on magnetic stirrer for adsorption of dyes till equilibrium was obtained. The aliquots were collected after filtration and un-adsorbed adsorbate concentration was determined using UV-Vis Spectrophotometer. Further, the optimized concentration of the solution was utilized for subsequent experiments. To determine the optimum quantity of FVSB utilized further in experiments, the range of 25- 200 mg of FVSB was added individually in optimum concentration (100 mg/L) of prepared MB and RB solutions. For optimum pH investigation, the adsorption process was performed with varying pH range of 2-12 until equilibrium was obtained. NaOH and HCl were used for adjustment of pH. All the solutions were placed on shaker for 420 minutes at room temperature (other than temperature variation study) with 160 rpm shaking speed to attain equilibrium condition. The filtered supernatant was analyzed on UV-visible spectrophotometer within the 400-800 nm range for concentration determination. With the help of optimized condition, at different time interval kinetics experiments were performed. 25 °C to 45 °C was the temperature range selected for the study of temperature variation effect on adsorption process. Each experiment of adsorption parameter was performed in triplicates and mean values were reported. Calculation of adsorption capacity, removal percentage as well as adsorption at particular time '*t*' was done using the following equations[36]:

$$q_e = \frac{(C_0 - C_e)}{m} * V \ldots\ldots\ldots\ldots\ldots (1)$$

$$\%R_e = \frac{C_0 - C_e}{C_e} * 100 \ldots\ldots\ldots\ldots (2)$$

$$q_t = \frac{(C_0 - C_t)}{m} * V \ldots\ldots\ldots\ldots\ldots (3)$$

where,

'q_e', '*%Re*' and 'q_t' denotes adsorption capacity (mg/g), removal efficiency of dyes and adsorption capacity at particular time '*t*' (mg/g), respectively. 'C_0' and 'C_e' is initial concentration (mg/L) and equilibrium concentration (mg/L). C_t represents the concentration of

dyes in aqueous solution at time '*t*' (mg/L); '*V*' and '*m*' represents solution volume (L) and weight of the adsorbent (g).

5.1.2.5. Simultaneous Adsorption of MB and RB

To investigate simultaneous adsorption, the binary system of MB and RB was used for adsorption study considering the practical relevance. 50 mL of 100 mg/L MB and RB solutions were taken for adsorption of binary system in the ratio of 1:1 using FVSB. The set up was kept on magnetic stirrer till equilibrium condition was attained and resultant were observed under UV-visible spectrophotometer.

5.1.2.6. Desorption Experiment and Reusability

Desorption experiment was performed using FVSB (100 mg) in 100 mg/L solution of MB and RB individually and stirred for 420 minutes till equilibrium. Solutions were filtered for concentration determination. Further, dye loaded FVSB was utilized for desorption study stirring continuously with 0.1 M HCl as desorbing agent. Regenerated FVSB were washed extensively with distilled water, dried and stored for next batch adsorption. Following equation was used for calculation of desorption efficiency (4)[37]

$$\boldsymbol{Desorption\ Efficiency} = \frac{\boldsymbol{Amount\ of\ Pollutant\ Desorbed}}{\boldsymbol{Amount\ of\ Pollutant\ Adsorbed}} \times \mathbf{100} \ \boldsymbol{\ldots\ldots\ (4)}$$

5.1.3. Results and Discussion

5.1.3.1.Characterization of Bioadsorbent

5.1.3.1.1. FTIR Spectra Analysis

FTIR spectra of FVSB were analyzed before and after adsorption of dyes MB and RB within the range of 500-4000 cm^{-1} (**Figure 5.1.2)**. The spectra of native bioadsorbent and dye loaded bioadsorbent exhibits same pattern with some changes. The hydroxyl (-O-H) and amine group (-N-H) presence was represented by broad band between the ranges of 3200-3500 cm^{-1}. The –C-H bond was represented by the peak of 2935 cm^{-1} associated with stretching vibration of alkyl groups. The peak at 1242 corresponds to presence of sulfur groups probably due to presence of fucoidan component in seaweed[38]. The sharp peak around 1600 cm^{-1} represents –C=O group of carboxylates and 1057 cm^{-1} shows –C-O stretching vibration carboxyl groups[34]. 1418 cm^{-1} is associated with –C-H as well as primary and secondary amines representing the presence of

lipids and proteins[30]. It was discovered that after adsorption process the functional groups shifted from 3343 to 3304 (for MB) and 3408 (for RB); 1644 to 1649 (for MB) and 1645 (for RB); 1533 to 1537 (for MB) and 1549 (for RB). The shifting confirms their participation in adsorption of dyes on FVSB.

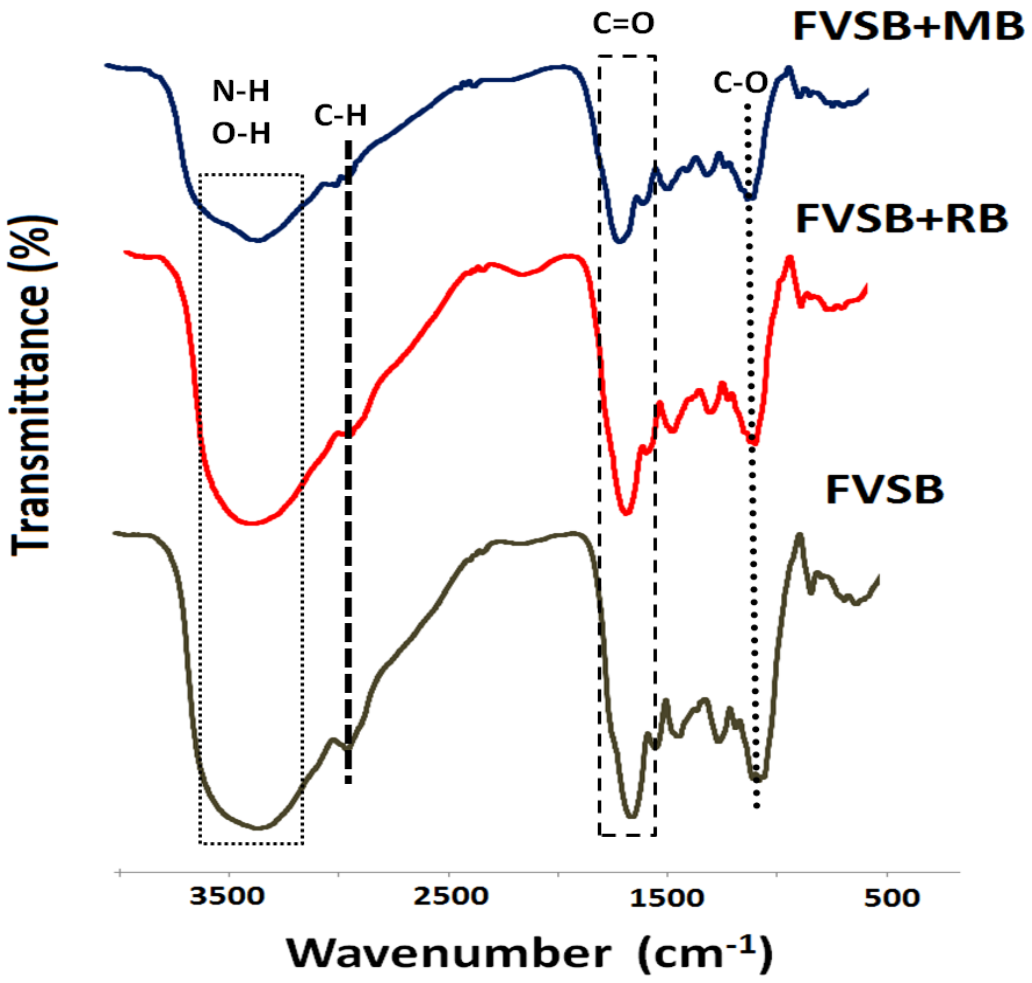

Figure 5.1.2: FTIR spectra of FVSB, FVSB+MB and FVSB+RB

5.1.3.1.2. SEM-EDX Analysis

Scanning Electron Microscope coupled with Energy Dispersive Spectrometer was utilized for the investigation of elemental composition and surface morphology of FVSB as well as dye loaded seaweed **Figure 5.1.3**. SEM analysis of FVSB represents a rough surface with different size and shapes of pores contributing to larger surface area for interaction of dyes[39]. The

adsorption of dyes (MB and RB) on the surface of FVSB smoothens the surface as shown in **Figure 5.1.3 (I).** EDS analysis of seaweed measure the elemental composition before and after adsorption. The results represent that FVSB dominates in carbon and oxygen content (**Figure 5.1.3 (II)**). After adsorption, increase in carbon percentage, decreasing oxygen content and the addition of nitrogen content shows the successful adsorption of MB and RB on surface of FVSB. The elements corresponding to molecules of adsorbate appear in the spectra of EDS showing transfer of dyes from solution to FVSB as shown in **Table 5.1.1**.

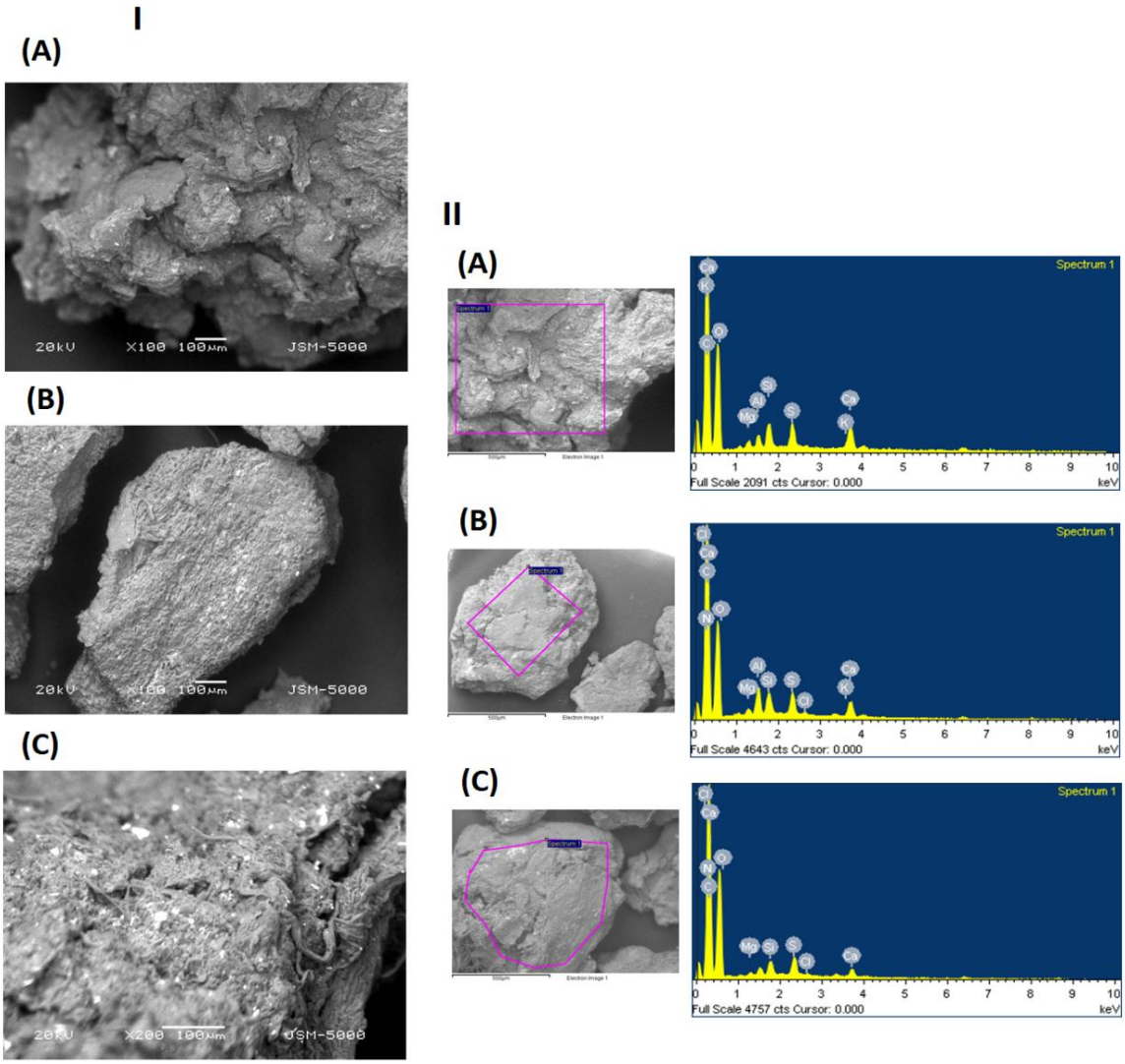

Figure 5.1.3: (I) SEM images of (A) FVSB, (B) FVSB+MB and (C) FVSB+RB; (II) EDS curves of (A) FVSB, (B) FVSB+MB and (C) FVSB+RB

Table 5.1.1: Elemental composition of FVSB before and after adsorption of MB and RB

Material	C (wt-%)	N (wt-%)	O (wt-%)	Mg (wt-%)	Al (wt-%)	S (wt-%)	Si (wt-%)
FVSB	*48.67*	*0.05*	*43.64*	*0.48*	*0.66*	*1.33*	*1.31*
FVSB+MB	*51.53*	*2.44*	*41.63*	*0.44*	*1.46*	*1.34*	*1.16*
FVSB+RB	*59.96*	*1.06*	*38.45*	*0.10*	*0*	*0.05*	*0.38*

5.1.3.1.3. TGA Analysis

Thermogravimetric analysis (TGA) of FVSB was performed in order to explore the thermal property of bioadsorbent. The mass loss was observed in two stages as shown in **Figure 5.1.4**. The first stage mass loss of 12.3% was associated with the removal of residual moisture present in bioadsorbent within the range of 30 to 150 °C. The second stage of degradation occurs in the range of 150-500 °C corresponding to 49.8% mass loss due to the presence of volatile matters, carbohydrates, cellulose, hemicelluloses, minerals and lipid content of FVSB[40].

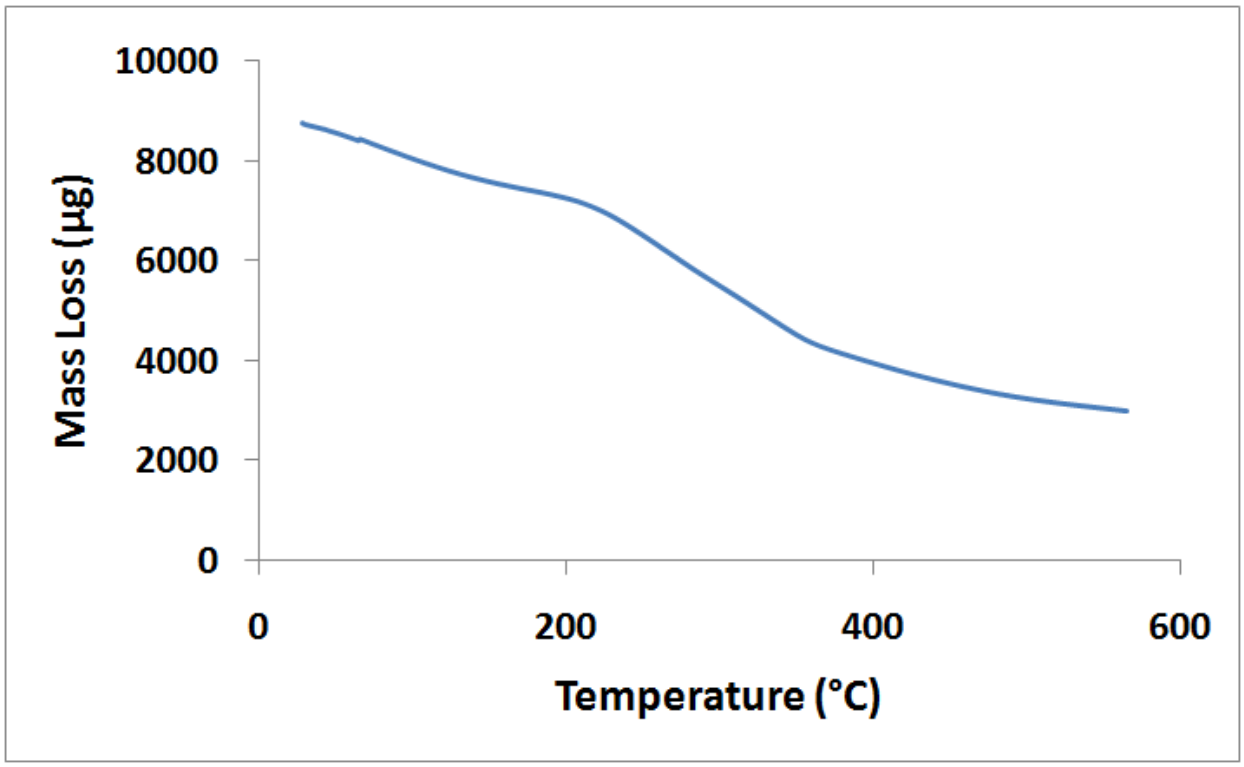

Figure 5.1.4: Thermogravimetric curves for FVSB

5.1.3.2. Effect of FVSB Dosage

One of the significant parameters related to adsorption process is the quantity of adsorbent which is directly related to vacant active sites. Increase in adsorbent quantity increases functional groups as well as active sites ultimately enhancing the removal efficiency of dyes. The same trend was observed in this case wherein removal efficiency increases with increasing adsorbent quantity (**Figure 5.1.5**). According to the results obtained, enhancement of removal efficiency is from 66.06% to 98.96% for MB and 75.31% to 95.14% for RB as the quantity of FVSB increased from 25 mg to 200 mg. 100 mg was considered as an optimum quantity in the adsorption process of MB and RB dyes.

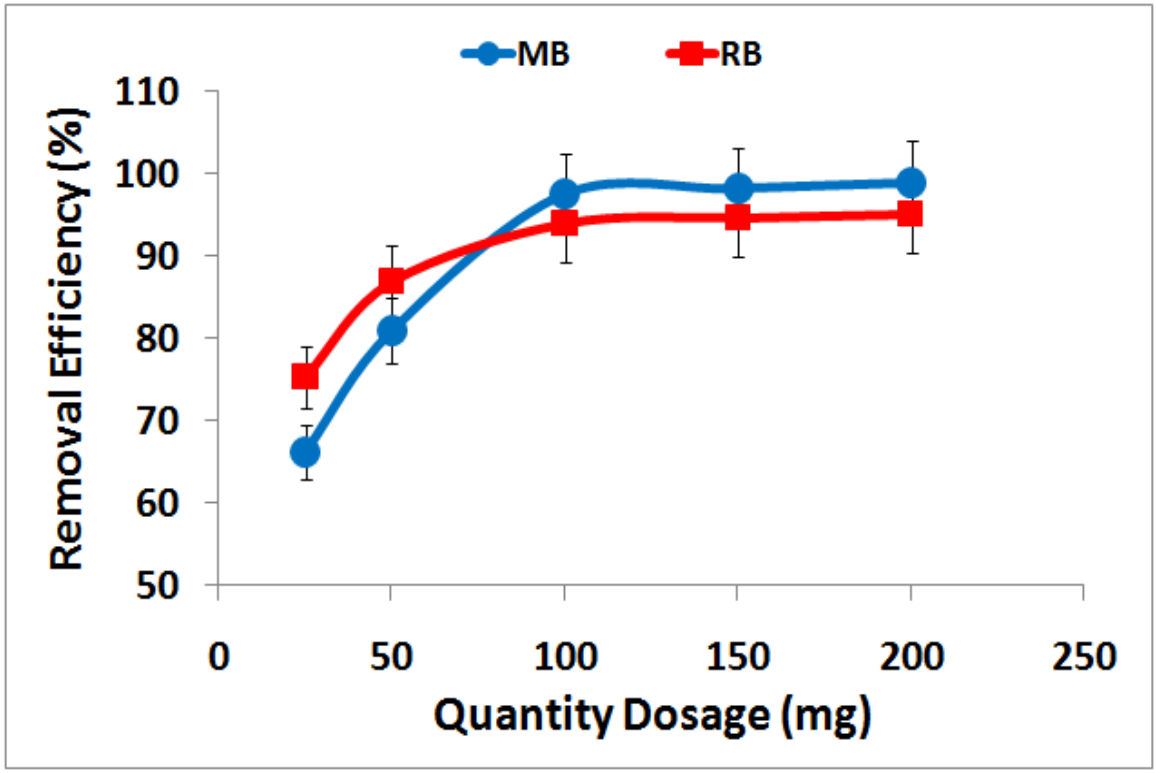

Figure 5.1.5: Effect of FVSB dosage on the percentage removal of 100mg/L of MB and RB at room temperature

5.1.3.3. Effect of Initial Concentration

Initial concentration of dyes has significant impact on removal efficiency and adsorption capacity in process of adsorption. For this study, the concentration range of adsorbate was 50 mg/L to 250 mg/L as shown in **Figure 5.1.6**. Results obtained from investigation exhibits increasing adsorption capacity from 48.9 to 185.68 mg/g and 47.67 to 158.38 mg/g for MB and

RB, respectively. The removal efficiency decreases from 97.81 to 74.27% and 95.35 to 63.35% for MB and RB, respectively, with an increment of initial concentration of dyes from 50 to 250 mg/L. Mass transfer gradient initiates dye molecules transfer from solution onto the surface of bioadsorbent. After optimum uptake of solute molecules, the removal efficiency decreases with increasing initial concentration due to repulsive forces between dye molecules of bulk solution and those present on bioadsorbent surface. In general, the adsorption dynamic exhibits various adsorption steps to transfer to solute such as particles diffusion i.e. adsorption of adsorbate into interior region of adsorbent, film diffusion like adsorption of adsorbate molecules from solution to the outer surface of adsorbent as well as the movement of adsorbate on interior surface of absorbent pores [41]. The rapid uptake of dyes in lower concentration shows maximum removal efficiency, therefore, 100 mg/L was considered as an optimum concentration for the adsorption study with removal efficiencies of 97.14 and 94.03% for MB and RB, respectively. The decreasing free active sites of adsorption and saturated condition does not favor further adsorption and results in decreasing nature of graph [42,43]

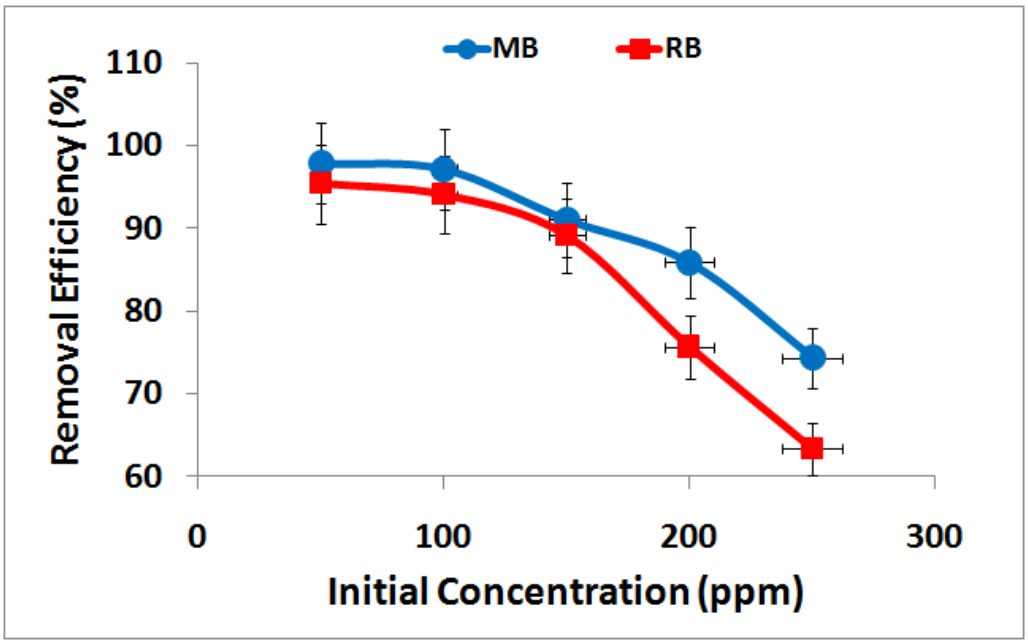

Figure 5.1.6: Effect of initial concentration of MB and RB on adsorption capacity and removal efficiency using FVSB at room temperature

5.1.3.4. Effect of pH

The initial pH is an important factor affecting the process of adsorption directly. The influence of initial pH on adsorption of MB and RB was explored in the range of 2-12. Several factors such

as change of the adsorbate degree of ionization, functional group dissociation level on active sites with bioadsorbent and charges affiliated with bioadsorbent surface[44]. MB shows maximum removal efficiency at higher pH and RB shows maximum removal in acidic pH. At basic pH the negatively charged functional groups on surface of bioadsorbent promotes the adsorption of MB dye. The presence of H^+ ions in acidic condition competes with MB molecules on surface of adsorbent[45]. Therefore, the removal efficiency increases from 34.35% to 98.01% with increasing pH. In case of RB, the maximum removal efficiency was observed at pH 4 i.e. 94.07% and minimum removal efficiency was observed at pH 12 i.e. 60.74% (**Figure 5.1.7)**. Cationic and monomeric forms of RB exist in acidic condition, due to which removal efficiency is higher in acidic pH. The change in pH forms different ionic species, mainly zwitterionic form at pH higher than 4. The formation of dimer due to the interaction of carboxyl and xanthene groups of RB reduces the removal efficiency of RB at higher pH. The optimum pH for MB adsorption is considered as 8 with removal efficiencies of 97.14% as no significant increase in removal efficiency was observed with raising pH, whereas the optimum pH for RB adsorption was considered as pH 6. The same pattern of adsorption of RB with maximum removal efficiency between pH 3 to 4 was previously reported[46].

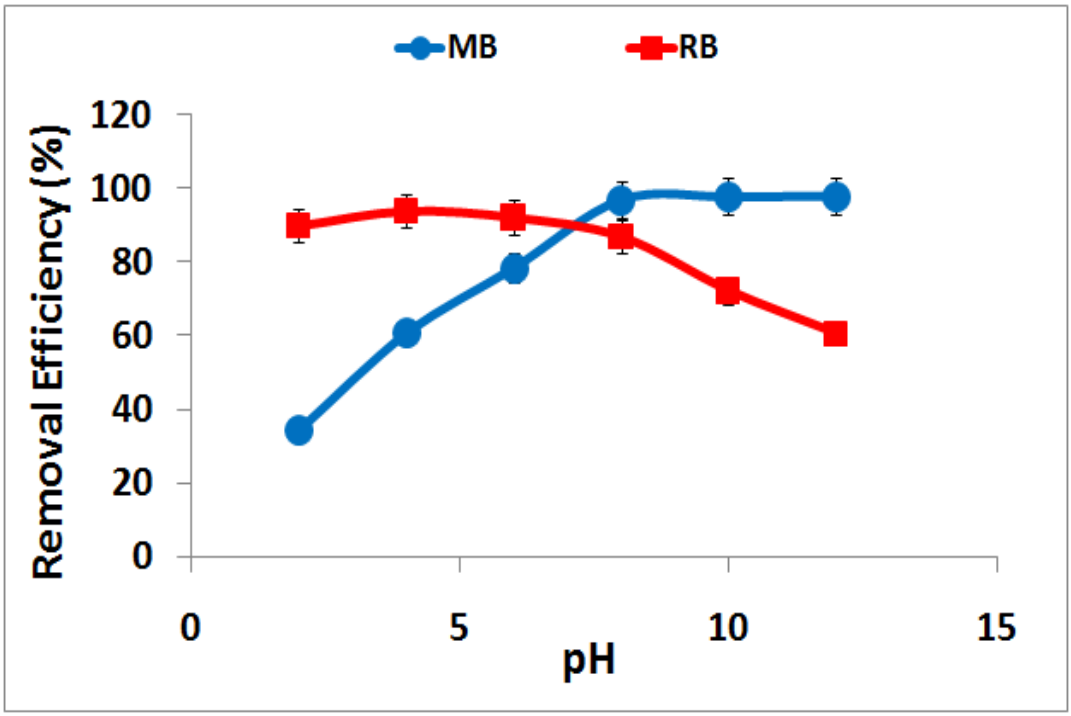

Figure 5.1.7: Effect of pH on removal efficiency of MB and RB on FVSB at room temperature

5.1.3.5. Effect of Contact Time

The effect of contact time on adsorption of dyes using FVSB at 60, 120, 180, 300 and 420 minutes has been represented in **Figure 5.1.8.** The pH of MB was fixed at 8 and for RB the pH was fixed at 4. After 420 minutes, the removal efficiency of MB and RB was observed as 95.13% and 93.44%, respectively. The presence of many unoccupied active sites results in rapid adsorption during initial phase as dye molecules interact with surface of bioadsorbent. Very slow adsorption was observed in between 300 to 420 minutes as active sites become saturated as well as difficult to be captured by adsorbate molecules; already present dye molecules on bioadsorbent surface repel those present in solution. The hydrogen bonding and electrostatic interaction are the two major processes that facilitate adsorption of dyes on FVSB. The trend of initial rapid increase and later constant removal efficiency has been reported [20,47].

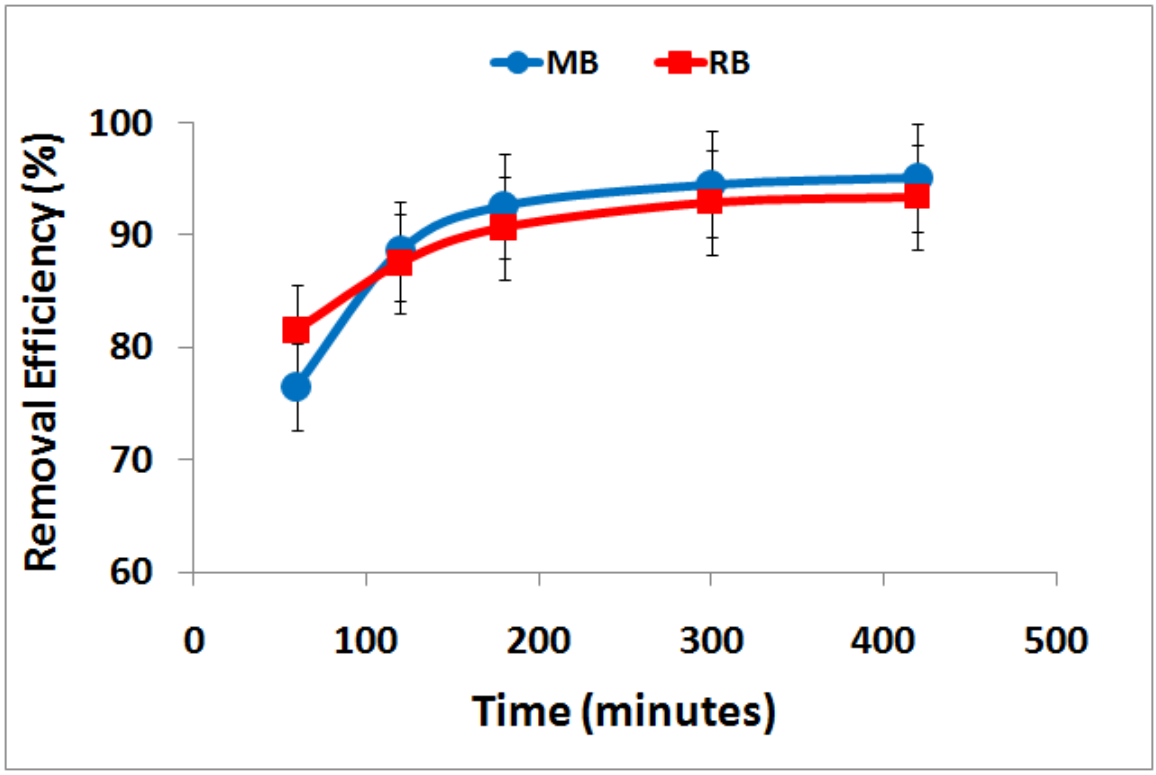

Figure 5.1.8: Effect of contact time on the percentage removal of 100mgL^{-1} of MB and RB at pH-8.0 and pH- 4.0, respectively at room temperature

5.1.3.6. Effect of Temperature

The increasing and decreasing removal efficiencies of dyes are directly affected by temperature variation. In this study of MB and RB adsorption on FVSB, the removal efficiency increases

with raising temperature range 25°C to 45°C as represented in **Figure 5.1.9**. The removal efficiency increases from 97.21 to 98.71% in case of MB and 93.57 to 96.68% in RB with increasing temperature. This adsorption study is favored at higher temperature; therefore the process of adsorption of dyes on FVSB is endothermic in nature. Temperature enhancement increases the adsorbate molecules mobility and also provides enough energy for interaction of adsorbate molecules and bioadsorbent surface [48]. A similar trend was also observed in some reported works of adsorption[20,37] .

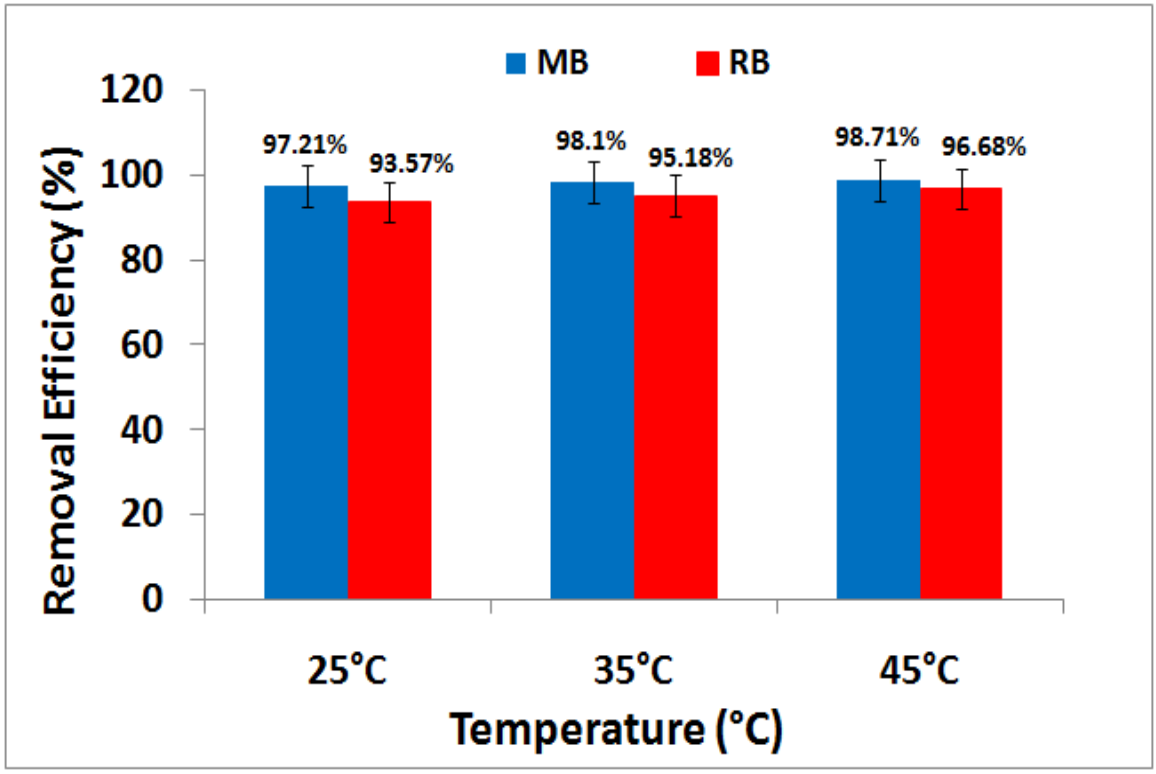

Figure 5.1.9: Effect of temperature on removal efficiency of MB and RB with increasing temperature from 25 °C to 45 °C

5.1.3.7. Adsorption Isotherms

The equilibrium adsorption isotherm is one of the significant aspects used in designing adsorption system for interpretation of adsorbate and adsorbent interaction, data analysis as well as adsorbent performance. Adsorption isotherm was represented as relationship of equilibrium concentration of adsorbate and equilibrium adsorption amount based on per unit gram of adsorbent. In this study, the Langmuir and Freundlich adsorption isotherm models were

investigated based on adsorption capacities of MB and RB. The following equation was utilized for evaluation of adsorption isotherm **(Figure 5.1.10)**.

$$\frac{Ce}{q_e} = \frac{1}{K_L} + \frac{Ce}{q_m} \ldots\ldots\ldots\ldots\ldots\ldots (5)$$

$$logq_e = logK_F + \frac{1}{n} logCe \ldots\ldots\ldots\ldots (6)$$

where, C_e (mg L^{-1}), q_e (mg g^{-1}), q_m (mg g^{-1}) represents equilibrium concentration of dyes, adsorption capacity of FVSB at equilibrium and maximum adsorption capacity, respectively. 1/n is constant affiliated with measurement of adsorbent and adsorbate relationship. K_L (L mg^{-1}) and K_F (L mg^{-1}) represents Langmuir equilibrium adsorption constant and Freundlich equilibrium adsorption constant, respectively. The value of K_L ($0 < K_L < 1$) shows the favorable condition, ($K_L > 1$) represents unfavorable condition and linear adsorption process was observed under the condition of ($K_L = 1$) [49].

Table 5.1.2 represents calculated values of Langmuir and Freundlich isotherm model. The experimental data was best fitted with Langmuir model with R^2 value of 0.998 and 0.999 for MB and RB. Since, the co-relation coefficient of Langmuir adsorption isotherm was higher than Freundlich adsorption isotherm therefore; representing Langmuir model accuracy i.e. monolayer adsorption of both dyes. In this model, homogenous spreading of active sites on the bioadsorbent surface was assumed. It could be concluded that, adsorption of both MB and RB shows monolayer coverage on energetically identical binding sites of FVSB [33,50].

Table 5.1.2: Adsorption isotherm constants for 100 mgL^{-1} of MB and RB at room temperature

Dye Molecule	Langmuir			Freundlich		
	q_m (mg g^{-1})	K_L (L mg^{-1})	R^2	1/n	K_F (L mg^{-1})	R^2
Methylene Blue	200	0.25	0.998	0.312	57.14	0.918
Rhodamine B	166.66	0.206	0.999	0.307	45.91	0.854

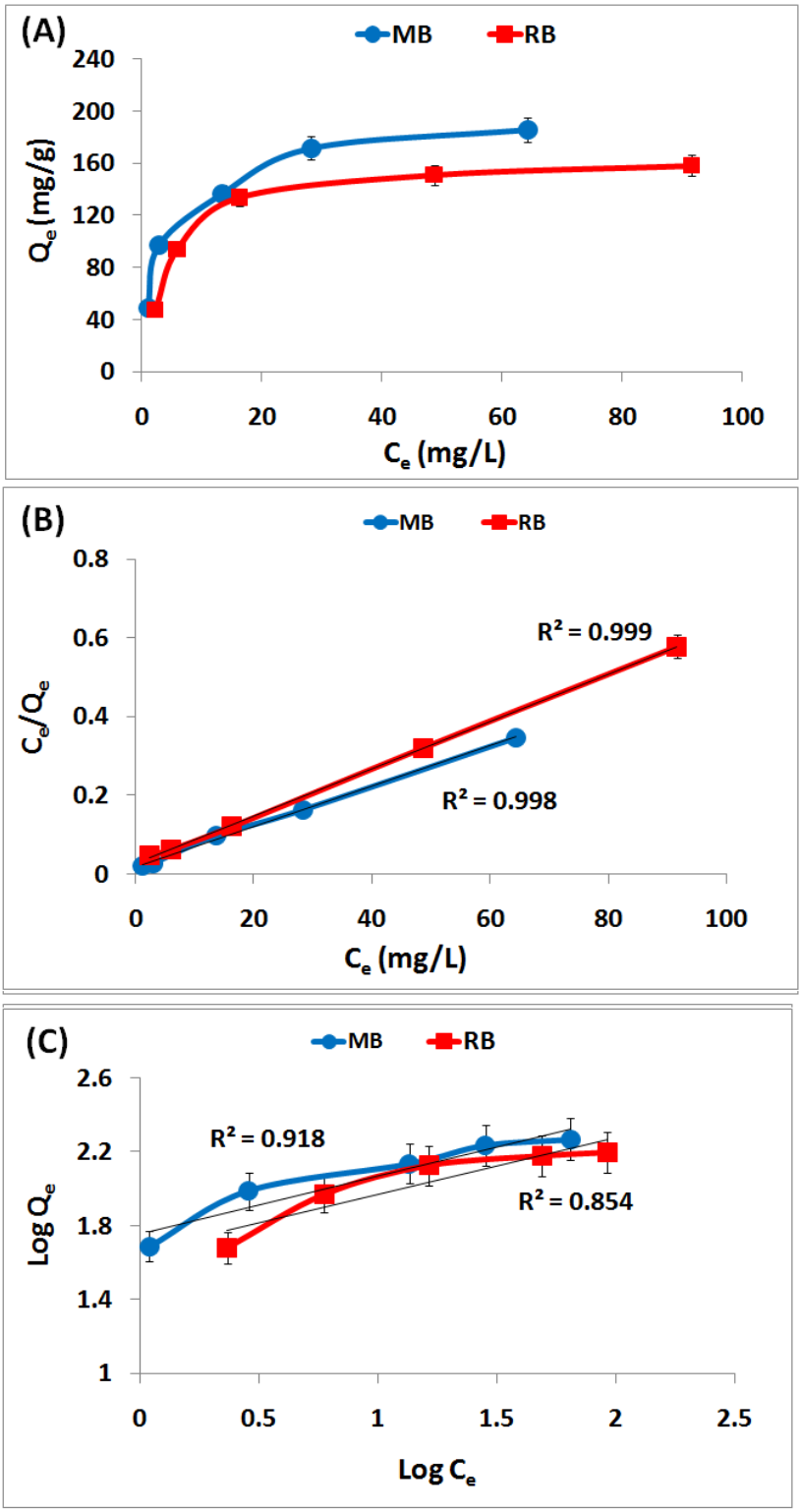

Figure 5.1.10: (A&B) Langmuir and (C) Freundlich adsorption isotherm for the removal of 100mgL^{-1} of MB and RB at room temperature

5.1.3.8. Adsorption Kinetics

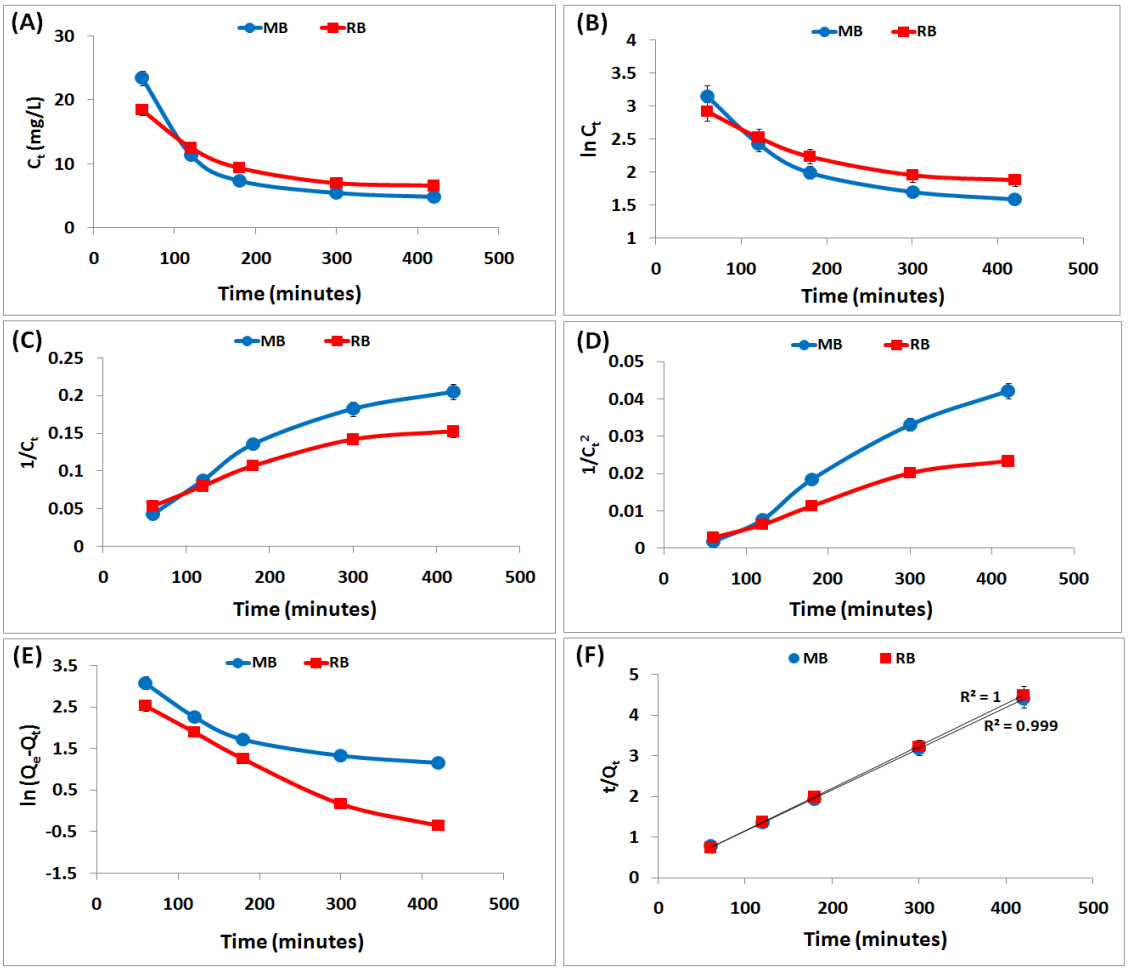

Figure 5.1.11: Graphs of (A) Zero order (B) First Order (C) Second Order (D) Third Order (E) Pseudo first order (F) Pseudo Second Order kinetic curve for MB and RB adsorption on FVSB

The time course trail was performed during adsorption of MB and RB for quantification of reaction time to reach equilibrium in mono-component solution system. It is a very significant factor for evaluation of designing process, practical applications and control of operation. The mechanism of adsorption as well as solute uptake has been described by adsorption kinetic models by managing dyes uptake time at the solid-solution interface. Zero order, First order, Second order, Third order, pseudo-first order and pseudo second order kinetic models were fitted

with experimental data to investigate the mechanism of adsorption. The following equations were utilized for calculation of adsorption kinetics parameters:

$$ln(q_e - q_t) = ln\, q_e - k_1 t \ldots\ldots\ldots\ldots\ldots\ldots\ldots (7)$$

$$\frac{t}{q_t} = \frac{1}{k_2 q_e^2} + \frac{t}{q_e} \ldots\ldots\ldots\ldots\ldots\ldots\ldots (8)$$

where, q_e and q_t (mg g^{-1}) shows amount of dyes adsorbed at equilibrium, is amount of dyes adsorbed at time t (minutes). k_1 is rate constant of pseudo-first order kinetic model while k_2 (mg min g^{-1}) is the rate constant of pseudo-second order kinetic model. Taking consideration of co-relation coefficient, the experimental data fitted best with pseudo- second order model as represented in **Figure 5.1.11**.

The co-relation coefficient of MB data was found to be 0.999 and for RB the R^2 value was 1. The adsorption kinetic parameters of MB and RB have been shown in **Table 5.1.3**. The experimental data follow pseudo-second order model, suggesting that adsorption of dyes are affiliated with their chemical interactions with FVSB surface and rate determining step is chemisorption.[51]

Table 5.1.3: Kinetic parameters for adsorption of MB and RB on FVSB

Pollutants	Pseudo First Order			Pseudo Second Order		
	Q_e (mg/g)	k_1 (10^{-5})	R^2	Q_e (mg/g)	k_2 (10^{-3})	R^2
MB	19.7	-1.2	0.84	100	0.67	0.999
RB	17.4	-1.9	0.97	100	0.88	1

5.1.3.9. Adsorption Thermodynamics

The spontaneity and mechanism of adsorption process is evaluated by adsorption thermodynamics parameter. Therefore, it has been considered as a significant parameter in adsorption study. The experimental data obtained from temperature variation of 25°C, 35°C and 45°C was taken into consideration for thermodynamic study. The Gibbs free energy ($\Delta G°$), Free energy change ($\Delta H°$) and entropy change ($\Delta S°$) are some parameters calculated from the slope

and intercept of a Vant Hoff plot of experimental data on K_C versus $1/T$ at various temperatures i.e. 298, 308 and 318 K (**Figure 5.1.12)**.

$$\Delta G° = -RT\,ln(K_c) \quad \text{..... (11)}$$

$$ln\,K_c = \frac{\Delta S°}{R} - \frac{\Delta H°}{R} \cdot \frac{1}{T} \quad \text{..... (12)}$$

where, 'K_c' is adsorption affinity i.e. Q_e/C_e, 'T' and 'R' is temperature (K) and gas constant (8.314 J.mol^{-1}. K^{-1})

The negative values of $\Delta G°$ obtained at various temperatures shows that the adsorption of MB and RB on FVSB is a spontaneous process. The increasing negative values of $\Delta G°$ with rising temperature suggest that process of adsorption is energetically favored. The parameter of thermodynamic study has been shown in **Table 5.1.4**. The endothermic nature of MB and RB adsorption with FVSB was represented by positive value of $\Delta H°$. Positive value of $\Delta S°$ represents enhancing randomness at the adsorbate/adsorbent interface during adsorption process. It has been reported that $\Delta H°$ value between 2.1–20.9 kJ mol^{-1} shows physisorption process, whereas in between 80-200 kJ mol^{-1} shows chemisorption. In this study, the calculated $\Delta H°$ value is more than 20.9, thus, chemisorption process facilitates adsorption of MB and RB onto FVSB. This trend is also supported by the kinetics modelling obtained as well as reported by other researchers. [52,53]

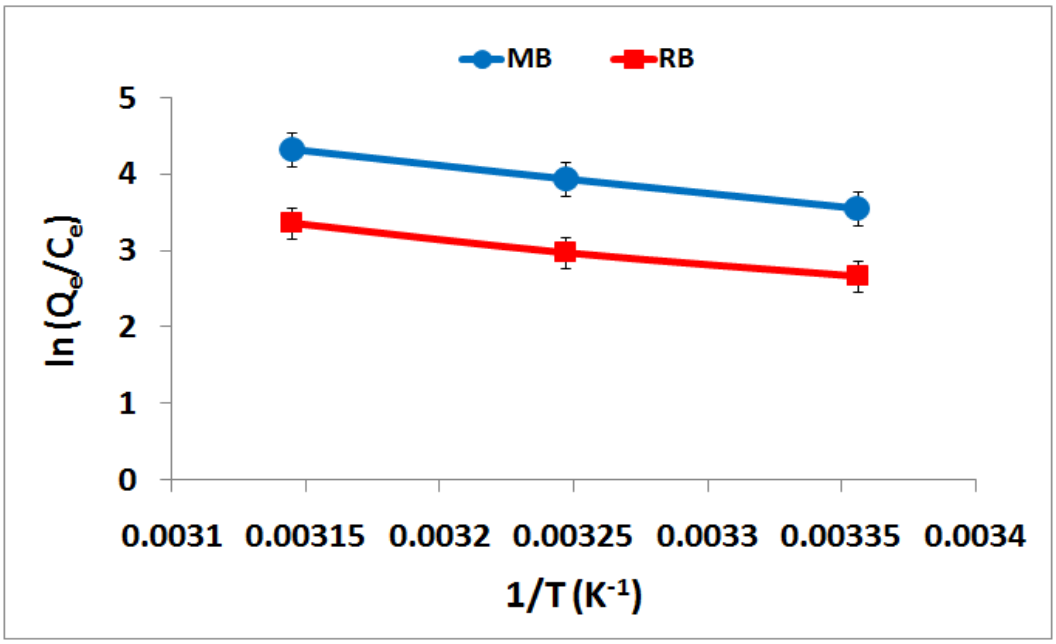

Figure 5.1.12: ln (Q_e/C_e) versus 1/T graph for estimation of thermodynamic parameters for adsorption of MB and RB on FVSB

Table 5.1.4: Thermodynamic parameters for the adsorption of MB and RB on FVSB

Contaminants	K_c			$\Delta H°$	$\Delta S°$	$\Delta G°$		
	298 K	308 K	318 K			298 K	308 K	318 K
MB	34.85	51.78	76.56	30.711	0.132	-8.79	-10.08	-11.44
RB	15.46	19.78	29.12	27.52	0.114	-6.61	-7.63	-8.90

5.1.3.10. Simultaneous Adsorption Study of MB and RB

The simultaneous adsorption of more than one dye increases the practical applicability of adsorbent. The result of simultaneous adsorption of MB and RB has been represented in **Figure 5.1.13**. For MB and RB, the removal efficiency was found to be 99.37% and 98.87% respectively in binary solution. The effect of simultaneous adsorption of dyes on FVSB was measured by utilizing the ratio of adsorption capacities (*Rq)*.

$$R_q = \frac{q_b, i}{q_m, i} \ldots\ldots\ldots\ldots\ldots\ldots (13)$$

where, q_m,*i* represents the adsorption capacity of component '*i'* in single system and q_b,*i* represents adsorption capacity of component '*i'* in binary system with same initial concentration. In general, three conditions are reported in case of simultaneous adsorption i.e. i) Synergism: the condition occurs when $R_q > 1$, where adsorption of one dye is escalated in the presence of another dye; ii) Antagonism: the condition occurs when $R_q < 1$, in this situation the adsorption of one dye is inhibited in presence of other dye and iii) Non-interaction: this condition occurs when $R_q = 1$, showing adsorption of one dye is unaffected by the presence of other dye. This study shows synergism, as $Rq > 1$ i.e. adsorption of dyes enhances in the presence of other dye[49]. Therefore, the FVSB synergistically facilitates the removal of both dyes in binary system. No antagonistic effect was observed during the process of adsorption when both dyes co-exist in mixture.

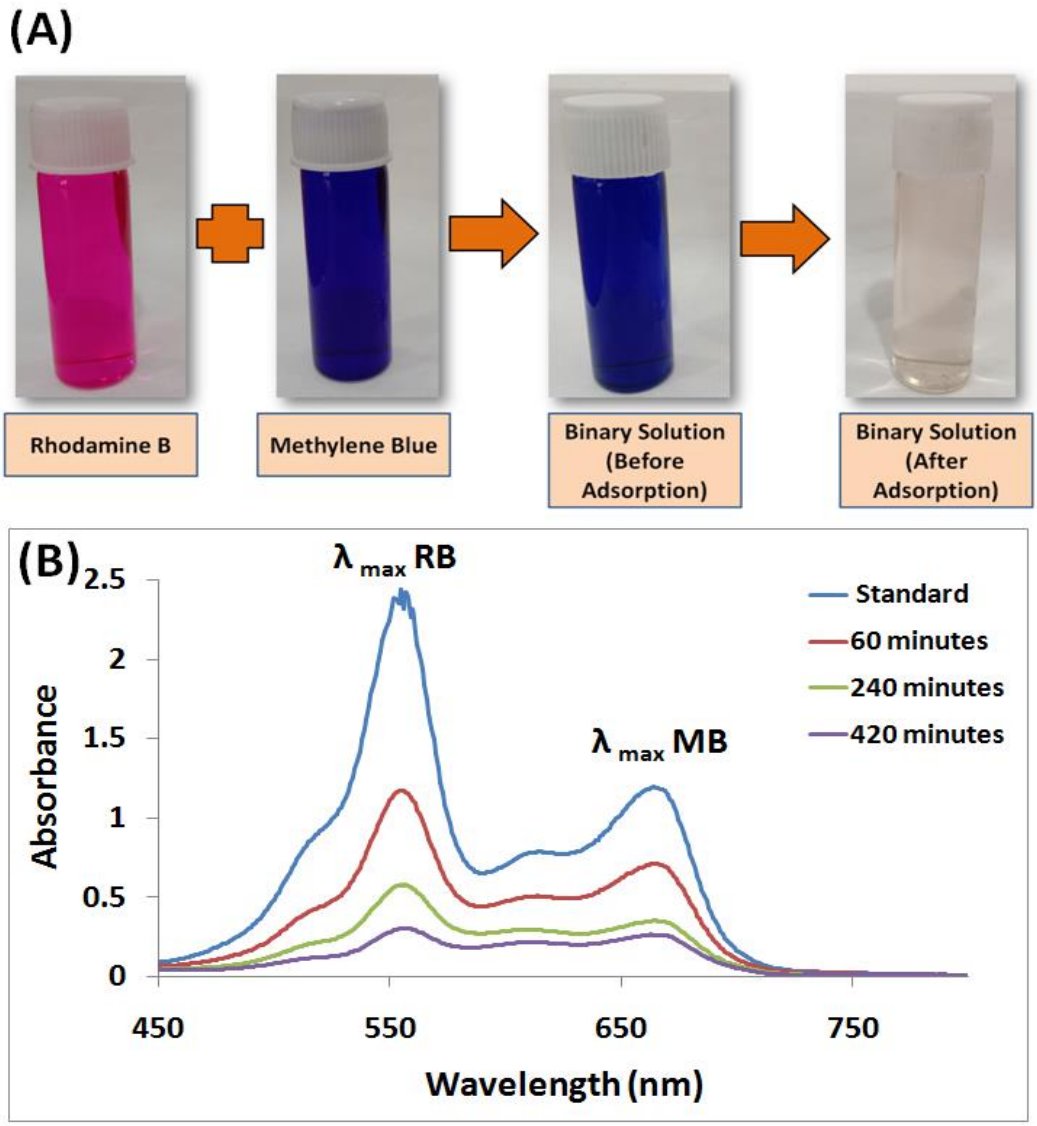

Figure 5.1.13: (A) Photographic images of binary solution before and after adsorption (B) UV-vis spectra of MB and RB in binary solution with time

5.1.3.11. Desorption and Regeneration

The important index considered for regeneration of bioadsorbent is desorption study that also helps in recovering adsorbate molecules. The efficiency and effectiveness of FVSB could be determined by desorption study. The suitable eluent system was selected based on the type of relationship occurring between adsorbent and adsorbate system. For assessment of regeneration and reusability of FVSB the consecutive adsorption and desorption cycle was executed using 0.1M HCl and 0.1M NaOH [54]. Since, better results were obtained with HCl therefore, it was used as eluent system for desorption cycle after washing with distilled water. The maximum removal

efficiency obtained after the first desorption cycle was 96.3% and 92.2% for MB and RB, respectively. As the **Figure 5.1.14 (A)** represents, the removal efficiency decreases slowly after every cycle reuse of FVSB. The FTIR spectra of FVSB after five adsorption cycles have shown that the structure of the bioadsorbent is not degraded or affected during the regeneration process. The outcomes exhibit that FVSB acquire significant reusability characteristics aiding to the economic viability of the process as shown in **Figure 5.1.14 (B)**. This suggests that FVSB retain their structure after successful adsorption of MB and RB.

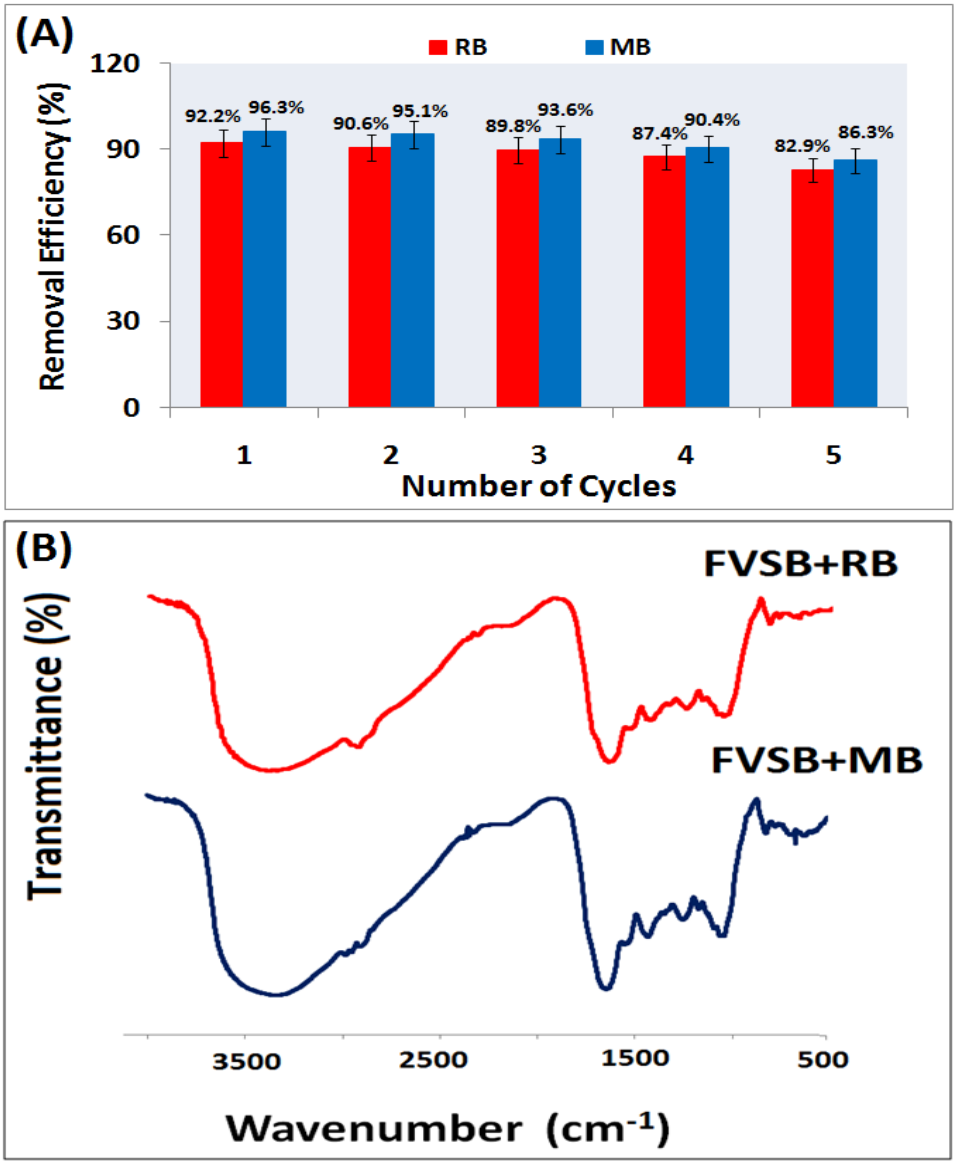

Figure 5.1.14: (A) Percentage removal of MB and RB after successive desorption/adsorption cycles using 0.1M HCl as eluent; (B) FTIR spectra of regenerated FVSB

5.1.3.12. Adsorption Mechanism

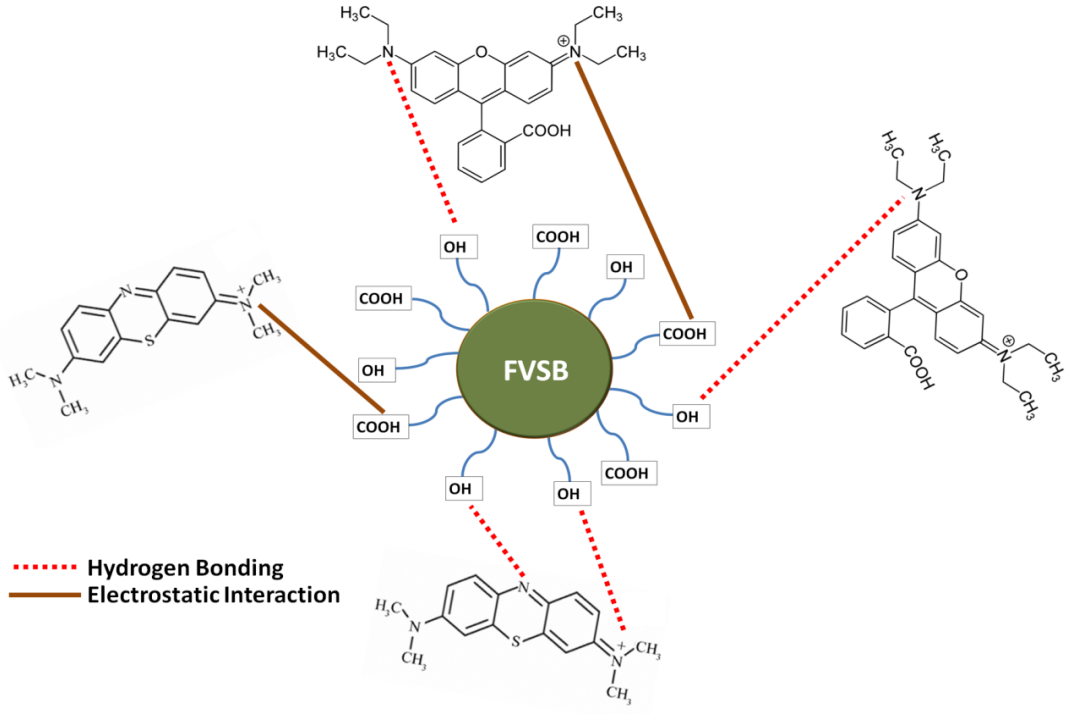

Figure 5.1.15: Probable mechanism of adsorption of MB and RB on FVSB

The plausible mechanism of MB and RB adsorption on FVSB has been represented in **Figure 5.1.15**. Various factors control and govern the process of adsorption; some of them are functional and structural behaviour of adsorbate molecules and several bioadsorbent surface characteristics like surface area, pore size, surface chemical groups, active sites etc. The adsorbate molecules of this system i.e. MB and RB are cationic dye pollutants. The surface of FVSB, contains several active functional groups like hydroxyl, carboxylic and amine groups that govern the process of adsorption. The MB and RB dye uptake was basically facilitated by the electrostatic interaction and hydrogen bonding between adsorbate and bioadsorbent surface. The FVSB could be considered as effective, sustainable and eco-friendly adsorbent system for efficiently removing the dyes from single and binary component system. The investigation of adsorption mechanism was done by using FTIR analysis. Before and after adsorption spectra of FVSB, helps in determining the interaction of dyes and surface of bioadsorbent. The slight shift of 2-4 cm^{-1} peaks of –O-H and –C=O confirms their contribution in adsorption mechanism. The decreasing intensity after adsorption represents the utilization of functional groups in adsorption process[33].

5.1.3.13. Adsorption of real sample using FVSB

The removal of color from real environmental sample has been investigated using textile effluent. The preliminary study of adsorption using FVSB has been done on real sample diluted in ratio 1:3. The 20 mL of diluted solution was investigated for adsorption study using 100 mg of FVSB for 420 minutes. The result shows decrease in color intensity visibly as well as supported by UV visible spectra of solutions before and after adsorption demonstrating successful environmental remediation process (**Figure 5.1.16**).

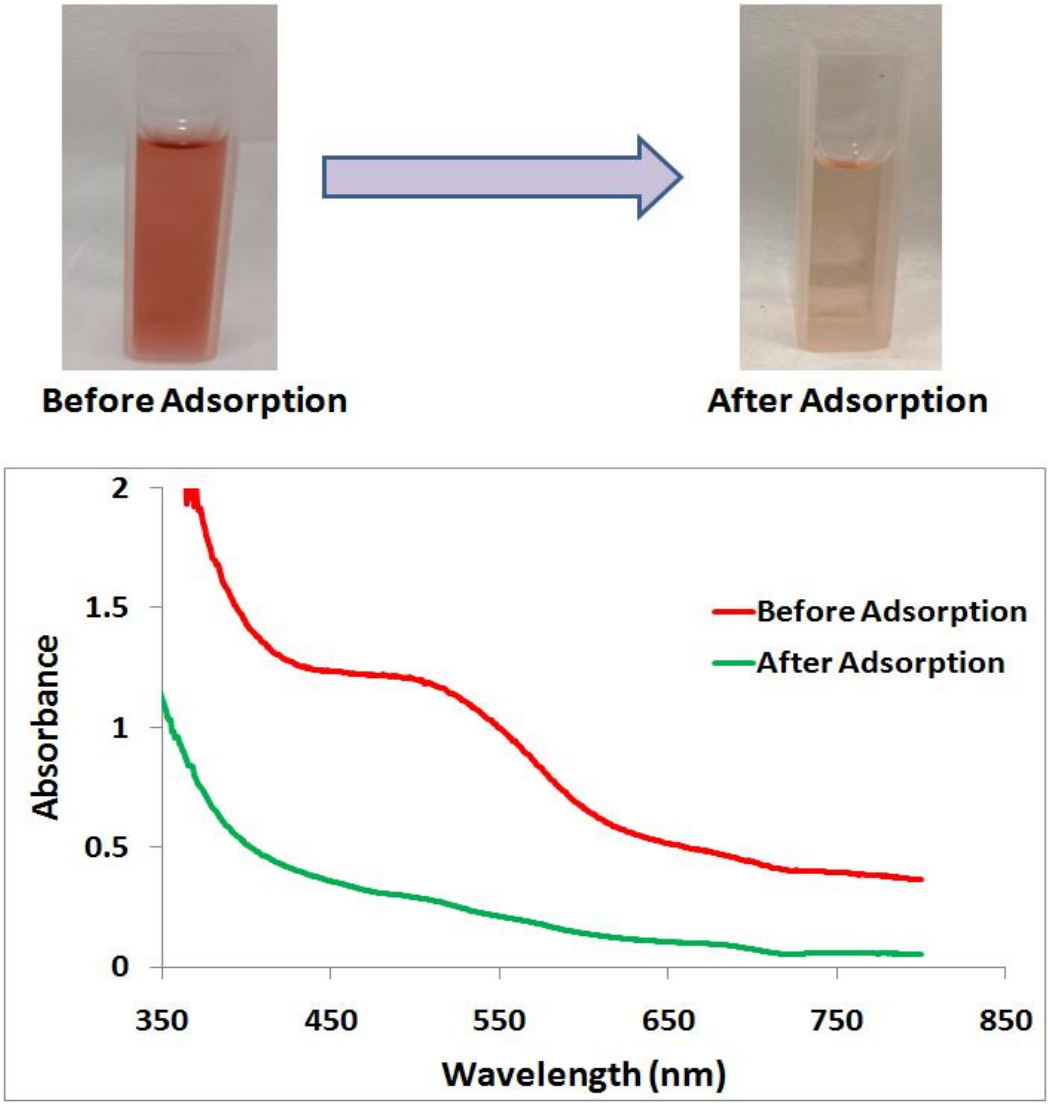

Figure 5.1.16: Photographic images and UV visible spectra of environmental sample adsorption using FVSB

5.1.3.14. Comparison with Other Adsorbents

The comparison table represents that maximum adsorption capacities of MB and RB obtained by using FVSB is better than other reported bioadsorbent (**Table 5.1.5**). FVSB could be regarded as preferable and promising bioadsorbent utilized for elimination of organic pollutants such as dyes from aqueous solution.

Table 5.1.5: Comparison of maximum adsorption capacities of FVSB with other adsorbents

Adsorbent	**Adsorbate**	**Q_m (mg/g)**	**Reference**
Ethanol modified *Gracilaria edulis* (EGE), Ethanol modified *Gracilaria salicornia* (EGS) and Ethanol modified *Kappaphycus alvarezii* (EKA)	RB	97.08 mg/g, 105.26 mg/g and 112 mg/g	[8]
magnetic iron oxide nanoparticles functionalized cress seed mucilage (CSM-MIONs)	MB	44.6 mg/g	[45]
Eucheuma cottonii seaweed biochar	MB	133.33 mg/g	[55]
Pomegranate peel	RB	30.47 mg/g	[53]
Casuarina equisetifolia needle (CEN)	RB	82.34 mg/g	[46]
waste seeds *Aleurites moluccana* (WAM)	MB, RB	178 mg/g and 117 mg/g	[56]
Activated carbon/cellulose composite (ACC) biosorbent	MB	103.66 mg/g	[57]
Banana Peels (BP), Cucumber Peels (CP) and Potato Peels (PP)	MB	211.9 mg/g, 179.9 mg/g and 107.2 mg/g	[58]
FVSB	MB and RB	200 mg/g and 166.6 mg/g	**This work**

5.1.4. Conclusion

In coastal region huge amount of seaweeds are available and implementation of biomass waste as bioadsorbent has been considered under this study. In summary, the present work investigated the adsorption of organic dyes i.e. MB and RB using *Fucus vesiculosus* seaweed bioadsorbent (FVSB). The FVSB is economically viable, efficient, sustainable, eco-friendly and easily available approach of pollutant removal. The removal efficiency of MB and RB was found to be 98.71% and 96.68%, respectively. The results obtained from adsorption process represented efficient adsorption capacity of 200 mg/g for MB and 166.66 mg/g for RB. The investigation of various adsorption parameters includes adsorbent dose, concentration, pH as well as temperature variation. The Langmuir adsorption isotherm model fitted well with experimental data representing monolayer adsorption and follows the pseudo-second-order kinetic model exhibiting chemisorption mechanism for adsorption. The thermodynamic study exhibits spontaneous process of adsorption of dyes. The detailed observation revealed that adsorption of MB and RB on FVSB is governed by electrostatic interaction and hydrogen bonding. At last, the FVSB was regenerated and reutilized by using 0.1M L^{-1} HCl in desorption process. No significant decrease was observed up to five subsequent cycles. FVSB was successfully utilized for removal of color from environmental sample. Therefore, FVSB could be considered as promising and preferable bioadsorbent for removal of organic dyes and aiding the environmental remediation process.

References

(1) Subbaiah, V.; Yarramuthi, V.; Kim, Y.; Min, K.; Kim, D. Ecotoxicology and Environmental Safety Removal of Anionic Dyes (Reactive Black 5 and Congo Red) from Aqueous Solutions Using Banana Peel Powder as an Adsorbent. *Ecotoxicol. Environ. Saf.* **2018**, *148*, 601–607. https://doi.org/10.1016/j.ecoenv.2017.10.075.

(2) Yadav, M.; Das, M.; Bhatt, S.; Shah, P.; Jadeja, R.; Thakore, S. Rapid Selective Optical Detection of Sulfur Containing Agrochemicals and Amino Acid by Functionalized Cyclodextrin Polymer Derived Gold Nanoprobes. *Microchem. J.* **2021**, *169*, 106630. https://doi.org/10.1016/j.microc.2021.106630.

(3) Othman, N. H.; Alias, N. H.; Shahruddin, M. Z.; Abu Bakar, N. F.; Nik Him, N. R.; Lau, W. J. Adsorption Kinetics of Methylene Blue Dyes onto Magnetic Graphene Oxide. *J. Environ. Chem. Eng.* **2018**, *6* (2), 2803–2811. https://doi.org/10.1016/j.jece.2018.04.024.

(4) Kamranifar, M.; Khodadadi, M.; Samiei, V.; Dehdashti, B.; Sepehr, M. N.; Rafati, L.; Nasseh, N. Comparison the Removal of Reactive Red 195 Dye Using Powder and Ash of Barberry Stem as a Low Cost Adsorbent from Aqueous Solutions : Isotherm and Kinetic Study. *J. Mol. Liq.* **2018**, *255*, 572–577. https://doi.org/10.1016/j.molliq.2018.01.188.

(5) Chen, J.; Chen, H. Removal of Anionic Dyes from an Aqueous Solution by a Magnetic Cationic Adsorbent Modified with DMDAAC. *New J. Chem.* **2018**, *42* (9), 7262–7271. https://doi.org/10.1039/c8nj00635k.

(6) Taghvay, M.; Gholam, N.; Marandi, B.; Kurdtabar, M. Adsorption of Methylene Blue , Brilliant Green and Rhodamine B from Aqueous Solution Using Collagen-g-p (AA-Co-NVP)/ Fe 3 O 4 @ SiO 2 Nanocomposite Hydrogel. *J. Polym. Environ.* **2019**, *27*, 581–599. https://doi.org/10.1007/s10924-019-01372-8.

(7) Shooto, N. D.; Thabede, P. M.; Bhila, B.; Moloto, H.; Bobby Naidoo, E. Lead Ions and Methylene Blue Dye Removal from Aqueous Solution by Mucuna Beans (Velvet Beans) Adsorbents. *J. Environ. Chem. Eng.* **2019**, 103557. https://doi.org/10.1016/j.jece.2019.103557.

(8) Selvakumar, A.; Rangabhashiyam, S. Biosorption of Rhodamine B onto Novel

Biosorbents from Kappaphycus Alvarezii , Gracilaria Salicornia and Gracilaria Edulis *. *Environ. Pollut.* **2019**, *255*, 113291. https://doi.org/10.1016/j.envpol.2019.113291.

(9) Sahoo, S. K.; Hota, G. Surface Functionalization of GO with MgO/MgFe2O4binary Oxides: A Novel Magnetic Nanoadsorbent for Removal of Fluoride Ions. *J. Environ. Chem. Eng.* **2018**, *6* (2), 2918–2931. https://doi.org/10.1016/j.jece.2018.04.054.

(10) Shah, A.; Shah, M. Characterisation and Bioremediation of Wastewater: A Review Exploring Bioremediation as a Sustainable Technique for Pharmaceutical Wastewater. *Groundw. Sustain. Dev.* **2020**, *11*, 100383–100394. https://doi.org/10.1016/j.gsd.2020.100383.

(11) Qiao, K.; Tian, W.; Bai, J.; Wang, L.; Zhao, J.; Song, T.; Chu, M. Removal of High-Molecular-Weight Polycyclic Aromatic Hydrocarbons by a Microbial Consortium Immobilized in Magnetic Floating Biochar Gel Beads. *Mar. Pollut. Bull.* **2020**, *159*, 111489. https://doi.org/https://doi.org/10.1016/j.marpolbul.2020.111489.

(12) Hu, X. S.; Liang, R.; Sun, G. Super-Adsorbent Hydrogel for Removal of Methylene Blue Dye from Aqueous Solution. *J. Mater. Chem. A* **2018**, *6* (36), 17612–17624. https://doi.org/10.1039/c8ta04722g.

(13) Li, D.; Li, Q.; Bai, N.; Dong, H.; Mao, D. One-Step Synthesis of Cationic Hydrogel for Efficient Dye Adsorption and Its Second Use for Emulsified Oil Separation. *ACS Sustain. Chem. Eng.* **2017**, *5* (6), 5598–5607. https://doi.org/10.1021/acssuschemeng.7b01083.

(14) Arumugam, N.; Chelliapan, S.; Kamyab, H.; Thirugnana, S.; Othman, N.; Nasri, N. S. Treatment of Wastewater Using Seaweed : A Review. *Int. J. Environ. Reserach Public Heal.* **2018**, *15*, 2851. https://doi.org/10.3390/ijerph15122851.

(15) El-Zahhar, A. A.; Awwad, N. S.; El-Katori, E. E. Removal of Bromophenol Blue Dye from Industrial Waste Water by Synthesizing Polymer-Clay Composite. *J. Mol. Liq.* **2014**, *199*, 454–461. https://doi.org/10.1016/j.molliq.2014.07.034.

(16) Gupta, V. K.; Agarwal, S.; Saleh, T. A. Synthesis and Characterization of Alumina-Coated Carbon Nanotubes and Their Application for Lead Removal. *J. Hazard. Mater.*

2011, *185* (1), 17–23. https://doi.org/10.1016/j.jhazmat.2010.08.053.

(17) Mittal, A.; Kaur, D.; Malviya, A.; Mittal, J.; Gupta, V. K. Adsorption Studies on the Removal of Coloring Agent Phenol Red from Wastewater Using Waste Materials as Adsorbents. *J. Colloid Interface Sci.* **2009**, *337* (2), 345–354. https://doi.org/10.1016/j.jcis.2009.05.016.

(18) Yang, S. T.; Chen, S.; Chang, Y.; Cao, A.; Liu, Y.; Wang, H. Removal of Methylene Blue from Aqueous Solution by Graphene Oxide. *J. Colloid Interface Sci.* **2011**, *359* (1), 24–29. https://doi.org/10.1016/j.jcis.2011.02.064.

(19) Valodkar, M.; Singh, P.; Jadeja, R. N.; Thounaojam, M.; Devkar, R.; Thakore, S. Cytotoxicity Evaluation and Antimicrobial Studies of Starch Capped Water Soluble Copper Nanoparticles. *J. Hazard. Mater.* **2012**, *202*, 244–249. https://doi.org/10.1016/j.jhazmat.2011.11.077.

(20) Liu, L.; Gao, Z.; Su, X.; Chen, X.; Jiang, L.; Yao, J. Adsorption Removal of Dyes from Single and Binary Solutions Using a Cellulose-Based Bioadsorbent. *ACS Sustain. Chem. Eng.* **2015**, *3* (3), 432–442. https://doi.org/10.1021/sc500848m.

(21) Nekouei, F.; Nekouei, S.; Tyagi, I.; Gupta, V. K. Kinetic, Thermodynamic and Isotherm Studies for Acid Blue 129 Removal from Liquids Using Copper Oxide Nanoparticle-Modified Activated Carbon as a Novel Adsorbent. *J. Mol. Liq.* **2015**, *201*, 124–133. https://doi.org/10.1016/j.molliq.2014.09.027.

(22) Hong, Y.; Kim, J.; Choi, A.; Pal, M.; Lee, G. RSC Advances Highly Stable Mesoporous Silica Nanospheres Embedded with FeCo / Graphitic Shell Nanocrystals as Magnetically Recyclable Multifunctional Adsorbents for Wastewater Treatment †. *RSC Adv.* **2017**, *8*, 1089–1097. https://doi.org/10.1039/C7RA12240C.

(23) Han, H.; Wei, W.; Jiang, Z.; Lu, J.; Zhu, J.; Xie, J. Removal of Cationic Dyes from Aqueous Solution by Adsorption onto Hydrophobic/Hydrophilic Silica Aerogel. *Colloids Surfaces A Physicochem. Eng. Asp.* **2016**, *509*, 539–549. https://doi.org/10.1016/j.colsurfa.2016.09.056.

(24) Saad, N.; Al-Mawla, M.; Moubarak, E.; Al-Ghoul, M.; El-Rassy, H. Surface-Functionalized Silica Aerogels and Alcogels for Methylene Blue Adsorption. *RSC Adv.* **2015**, *5* (8), 6111–6122. https://doi.org/10.1039/c4ra15504a.

(25) Wu, X.; Hui, K. N.; Hui, K. S.; Lee, S. K.; Zhou, W.; Chen, R.; Hwang, D. H.; Cho, Y. R.; Son, Y. G. Adsorption of Basic Yellow 87 from Aqueous Solution onto Two Different Mesoporous Adsorbents. *Chem. Eng. J.* **2012**, *180*, 91–98. https://doi.org/10.1016/j.cej.2011.11.009.

(26) Demarchi, C. A.; Chahm, T.; Martins, B. A.; Debrassi, A.; Nedelko, N.; Ślawska-Waniewska, A.; Dłuzewski, P.; Dynowska, E.; Greneche, J. M.; Rodrigues, C. A. Adsorption of Reactive Red Dye (RR-120) on Nanoadsorbent O-Carboxymethylchitosan/γ-Fe2O3: Kinetic, Equilibrium and Factorial Design Studies. *RSC Adv.* **2016**, *6* (41), 35058–35070. https://doi.org/10.1039/c6ra04249j.

(27) Guleria, A.; Kumari, G.; Lima, E. C. Cellulose-g-Poly-(Acrylamide-Co-Acrylic Acid) Polymeric Bioadsorbent for the Removal of Toxic Inorganic Pollutants from Wastewaters. *Carbohydr. Polym.* **2020**, *228*, 115396. https://doi.org/10.1016/j.carbpol.2019.115396.

(28) Mallampati, R.; Xuanjun, L.; Adin, A.; Valiyaveettil, S. Fruit Peels as Efficient Renewable Adsorbents for Removal of Dissolved Heavy Metals and Dyes from Water. *ACS Sustain. Chem. Eng.* **2015**, *3* (6), 1117–1124. https://doi.org/10.1021/acssuschemeng.5b00207.

(29) Varma, R.; Turner, A.; Brown, M. T. Bioaccumulation of Metals by Fucus Ceranoides in Estuaries of South West England. *Mar. Pollut. Bull.* **2011**, *62* (11), 2557–2562. https://doi.org/10.1016/j.marpolbul.2011.08.016.

(30) Lebron, Y. A. R.; Moreira, V. R.; Santos, L. V. S. Studies on Dye Biosorption Enhancement by Chemically Modified Fucus Vesiculosus , Spirulina Maxima and Chlorella Pyrenoidosa Algae. *J. Clean. Prod.* **2019**, *240*, 118197. https://doi.org/10.1016/j.jclepro.2019.118197.

(31) Brinza, L.; Geraki, K.; Breaban, I. G.; Neamtu, M. Zn Adsorption onto Irish Fucus Vesiculosus: Bioadsorbent Uptake Capacity and Atomistic Mechanism Insights. *J.*

Hazard. Mater. **2018**, *365*, 252–260. https://doi.org/10.1016/j.jhazmat.2018.11.009.

(32) Thivya, J.; Vijayaraghavan, J. Single and Binary Sorption of Reactive Dyes onto Red Seaweed-Derived Biochar : Multi-Component Isotherm and Modelling. *Desalin. Water Treat.* **2019**, *156*, 87–95. https://doi.org/10.5004/dwt.2019.23974.

(33) Oualid, H. A.; Abdellaoui, Y.; Laabd, M.; Ouardi, M. El; Brahmi, Y.; Iazza, M.; Oualid, J. A. Eco-Efficient Green Seaweed Codium Decorticatum Biosorbent for Textile Dyes : Characterization , Mechanism , Recyclability , and RSM Optimization. *ACS Omega* **2020**, *5*, 22192–22207. https://doi.org/10.1021/acsomega.0c02311.

(34) El Atouani, S.; Belattmania, Z.; Reani, A.; Tahiri, S.; Aarfane, A.; Bentiss, F.; Jama, C.; Zrid, R.; Sabour, B. Brown Seaweed Sargassum Muticum as Low-Cost Biosorbent of Methylene Blue. *Int. J. Environ. Res.* **2019**, *13* (1), 131–142. https://doi.org/10.1007/s41742-018-0161-4.

(35) Jadeja, R. N.; Batty, L. Metal Content of Seaweeds in the Vicinity of Acid Mine Drainage in Amlwch, North Wales, U.K. *Indian J. Geo-Marine Sci.* **2013**, *42* (1), 16–20.

(36) Ebadi, A.; Rafati, A. A. Preparation of Silica Mesoporous Nanoparticles Functionalized with β-Cyclodextrin and Its Application for Methylene Blue Removal. *J. Mol. Liq.* **2015**, *209* (1), 239–245. https://doi.org/10.1016/j.molliq.2015.06.009.

(37) Munagapati, V. S.; Kim, D. S. Adsorption of Anionic Azo Dye Congo Red from Aqueous Solution by Cationic Modified Orange Peel Powder. *J. Mol. Liq.* **2016**, *220*, 540–548. https://doi.org/10.1016/j.molliq.2016.04.119.

(38) Mokhtar, N.; Aziz, E. A.; Aris, A.; Ishak, W. F. W.; Mohd Ali, N. S. Biosorption of Azo-Dye Using Marine Macro-Alga of Euchema Spinosum. *J. Environ. Chem. Eng.* **2017**, *5* (6), 5721–5731. https://doi.org/10.1016/j.jece.2017.10.043.

(39) Shakoor, S.; Nasar, A. Removal of Methylene Blue Dye from Artificially Contaminated Water Using Citrus Limetta Peel Waste as a Very Low Cost Adsorbent. *J. Taiwan Inst. Chem. Eng.* **2016**, *66*, 154–163. https://doi.org/10.1016/j.jtice.2016.06.009.

(40) Moreira, V. R.; Lebron, Y. A. R.; Lange, L. C.; Santos, L. V. S. Simultaneous Biosorption

of Cd (II), Ni (II) and Pb (II) onto a Brown Macroalgae Fucus Vesiculosus : Mono- and Multi-Component Isotherms , Kinetics and Thermodynamics. *J. Environ. Manage.* **2019**, *251*, 109587. https://doi.org/10.1016/j.jenvman.2019.109587.

(41) Isaac, C. P. J.; Sivakumar, A. Removal of Lead and Cadmium Ions from Water Using Annona Squamosa Shell: Kinetic and Equilibrium Studies. *Desalin. Water Treat.* **2013**, *51* (40–42), 7700–7709. https://doi.org/10.1080/19443994.2013.778218.

(42) Jalil, A. A.; Triwahyono, S.; Yaakob, M. R.; Azmi, Z. Z. A.; Sapawe, N.; Kamarudin, N. H. N.; Setiabudi, H. D.; Jaafar, N. F.; Sidik, S. M.; Adam, S. H.; et al. Utilization of Bivalve Shell-Treated Zea Mays L. (Maize) Husk Leaf as a Low-Cost Biosorbent for Enhanced Adsorption of Malachite Green. *Bioresour. Technol.* **2012**, *120*, 218–224. https://doi.org/10.1016/j.biortech.2012.06.066.

(43) Qi, X.; Wei, W.; Su, T.; Zhang, J.; Dong, W. Fabrication of a New Polysaccharide-Based Adsorbent for Water Purification. *Carbohydr. Polym.* **2018**, *195*, 368–377. https://doi.org/10.1016/j.carbpol.2018.04.112.

(44) Nandi, B. K.; Goswami, A.; Purkait, M. K. Adsorption Characteristics of Brilliant Green Dye on Kaolin. *J. Hazard. Mater.* **2009**, *161*, 387–395. https://doi.org/10.1016/j.jhazmat.2008.03.110.

(45) Allafchian, A.; Mousavi, Z. S.; Hosseini, S. S. Application of Cress Seed Musilage Magnetic Nanocomposites for Removal of Methylene Blue Dye from Water. *Int. J. Biol. Macromol.* **2019**, *136*, 199–208. https://doi.org/10.1016/j.ijbiomac.2019.06.083.

(46) Raziq, M.; Kooh, R.; Dahri, M. K.; Lim, L. B. L. The Removal of Rhodamine B Dye from Aqueous Solution Using Casuarina Equisetifolia Needles as Adsorbent The Removal of Rhodamine B Dye from Aqueous Solution Using Casuarina Equisetifolia Needles as Adsorbent. *Cogent Environ. Sci.* **2016**, *2*, 1140553. https://doi.org/10.1080/23311843.2016.1140553.

(47) Nawaz, H.; Zaman, Q.; Kausar, A.; Noreen, S.; Iqbal, M. Efficient Remediation of Zr (IV) Using Citrus Peel Waste Biomass : Kinetic , Equilibrium and Thermodynamic Studies. *Ecol. Eng.* **2016**, *95*, 216–228. https://doi.org/10.1016/j.ecoleng.2016.06.087.

(48) Aichour, A.; Zaghouane-boudiaf, H. Single and Competitve Adsorption Studies of Two Cationic Dyes from Aqueous Mediums onto Cellulose-Based Modified Citrus Peels/Calcium Alginate Composite. *Int. J. Biol. Macromol.* **2020**, *154*, 1227–1236. https://doi.org/10.1016/j.ijbiomac.2019.10.277.

(49) Das, M.; Yadav, M.; Shukla, F.; Ansari, S.; Jadeja, R. N.; Thakore, S. Facile Design of a Dextran Derived Polyurethane Hydrogel and Metallopolymer: A Sustainable Approach for Elimination of Organic Dyes and Reduction of Nitrophenols. *New J. Chem.* **2020**, *44* (44), 19122–19134. https://doi.org/10.1039/d0nj01871f.

(50) Maruthapandi, M.; Kumar, V. B.; Luong, J. H. T.; Gedanken, A. Kinetics , Isotherm , and Thermodynamic Studies of Methylene Blue Adsorption on Polyaniline and Polypyrrole Macro − Nanoparticles Synthesized by C - Dot-Initiated Polymerization. *ACS Omega* **2018**, *3*, 7196–7203. https://doi.org/10.1021/acsomega.8b00478.

(51) Yadav, M.; Das, M.; Savani, C.; Thakore, S.; Jadeja, R. Maleic Anhydride Cross-Linked β - Cyclodextrin-Conjugated Magnetic Nanoadsorbent : An Ecofriendly Approach for Simultaneous Adsorption of Hydrophilic and Hydrophobic Dyes. *ACS Omega* **2019**, *4*, 11993–12003. https://doi.org/10.1021/acsomega.9b00881.

(52) Das, S.; Dash, S. K.; Parida, K. M. Kinetics , Isotherm , and Thermodynamic Study for Ultrafast Adsorption of Azo Dye by an E Ffi Cient Sorbent : Ternary Mg /(Al + Fe) Layered Double Hydroxides. *ACS Omega* **2018**, *3*, 2532–2545. https://doi.org/10.1021/acsomega.7b01807.

(53) Ghibate, R.; Senhaji, O.; Taouil, R. Case Studies in Chemical and Environmental Engineering Kinetic and Thermodynamic Approaches on Rhodamine B Adsorption onto Pomegranate Peel. *Case Stud. Chem. Environ. Eng.* **2021**, *3*, 100078. https://doi.org/10.1016/j.cscee.2020.100078.

(54) Feng, Y.; Liu, Y.; Xue, L.; Sun, H.; Guo, Z.; Zhang, Y.; Yang, L. Carboxylic Acid Functionalized Sesame Straw : A Sustainable Cost-Effective Bioadsorbent with Superior Dye Adsorption Capacity. *Bioresour. Technol.* **2017**, *238* (50), 675–683. https://doi.org/10.1016/j.biortech.2017.04.066.

(55) Ameen, A.; Saeed, H.; Harun, N. Y.; Sufian, S.; Al-fakih, A.; Abdulhakim, A.; Ghaleb, S.; Almahbashi, N. Eucheuma Cottonii Seaweed-Based Biochar for Adsorption of Methylene Blue Dye. *Sustainability* **2020**, *12*, 10318.

(56) Postai, D. L.; Demarchi, C. A.; Zanatta, F.; Melo, D. C. C.; Rodrigues, C. A. Adsorption of Rhodamine B and Methylene Blue Dyes Using Waste of Seeds of Aleurites Moluccana , a Low Cost Adsorbent. *Alexandria Eng. J.* **2016**, *55*, 1713–1723. https://doi.org/10.1016/j.aej.2016.03.017.

(57) Somsesta, N.; Sricharoenchaikul, V.; Aht-Ong, D. Adsorption Removal of Methylene Blue onto Activated Carbon/Cellulose Biocomposite Films: Equilibrium and Kinetic Studies. *Mater. Chem. Phys.* **2020**, *240*, 122221. https://doi.org/10.1016/j.matchemphys.2019.122221.

(58) Stavrinou, A.; Aggelopoulos, C. A.; Tsakiroglou, C. D. Exploring the Adsorption Mechanisms of Cationic and Anionic Dyes onto Agricultural Waste Peels of Banana , Cucumber and Potato : Adsorption Kinetics and Equilibrium Isotherms as a Tool. *J. Environ. Chem. Eng.* **2018**, *6*, 6958–6970. https://doi.org/10.1016/j.jece.2018.10.063.